An Anatomy of Option Pricing Models

Nicole Branger[‡]

This version: December 8, 2004

[‡]Faculty of Economics and Business Administration, Goethe University, Mertonstr. 17, Uni-Pf 77, D-60054 Frankfurt am Main, Germany. E-mail: branger@wiwi.uni-frankfurt.de

I thank Christian Schlag for many valuable comments and suggestions and for stimulating discussions.

An Anatomy of Option Pricing Models

Abstract

This paper analyzes the properties of and the differences between derivative pricing models that include stochastic volatility or stochastic jumps or both of these risk factors. The focus is on the pricing of European options. In a first step, we discuss the impact of the parameters in stochastic volatility models and in jump-diffusion models, the characteristics of the implied volatility smile in these two models, and the main structural differences between stochastic volatility and stochastic jumps. In a second step, we consider models that combine the basic risk factors. We show which additional characteristics of option prices can be explained by models with both stochastic volatility and stochastic jumps. We also show that the use of two stochastic volatility processes allows to model a stochastic skew, which cannot be captured by the other models.

JEL: G12, G13

Keywords: Stochastic volatility, stochastic jumps, model specification, stochastic skew, implied volatilities, smile, term structure of implied volatilities

1 Introduction and Motivation

One of the most important issues in option pricing is model specification. Models discussed in the literature differ with respect to the risk factors they include. In the basic model of Black and Scholes (1973) (BS), there is only stock price risk, and the stock price follows a diffusion process with constant volatility. However, a large number of empirical studies has documented that this simple model cannot explain the option prices observed at the market, and that additional risk factors are reflected in these prices, see, for example, Bakshi, Cao, and Chen (1997), Coval and Shumway (2001), Buraschi and Jackwerth (2001), Pan (2002), Bakshi and Kapadia (2003), Eraker, Johannes, and Polson (2003), Eraker (2004), and Broadie, Chernov, and Johannes (2004).

The two most frequently discussed risk factors in addition to stock price risk are stochastic volatility (SV) and stochastic jumps (SJ). Examples for the first class of models include Hull and White (1987), Heston (1993), or Schöbel and Zhu (1999), while the most prominent model with stochastic jumps is the jump-diffusion model of Merton (1976). Models with both stochastic volatility and stochastic jumps (SVJ) were proposed by Bakshi, Cao, and Chen (1997) and Bates (1996). Duffie, Pan, and Singleton (2000) and Eraker (2004), among others, also include jumps in volatility. Bakshi, Cao, and Chen (1997) furthermore consider stochastic interest rates, but argue that this risk factor is much less important than SV and SJ. Other authors, like Carr and Wu (2004), rely on Lévy processes to model the behavior of stock prices.

When it comes to choosing one of these models, it is important to have an idea about their similarities and differences. What are the implications of using an SJ model instead of an SV model or vice versa, and what do we gain by using a more sophisticated model that includes several risk factors? In this paper, we answer these questions and provide a detailed analysis of models with SV, SJ, or both.

Models can differ in several dimensions. They can differ in pricing, in hedging, or in their implications concerning portfolio selection, to name just a few examples. The degree of diversity of two models thus also depends on the purpose we want to use them for and on the information available to identify them. For example, assume that two models give the same prices for a cross section of European options, but differ when it comes to pricing barrier options. If we only want to price European options, the differences between the models do not matter, whereas they become crucially important when exotic options are to be valued.

In this paper, we focus on the differences in pricing European options, and we discuss the properties of the implied volatility function for the different models. First, we provide a detailed analysis of SV and SJ models. We consider the two most prominent models, which are the SV model of Heston (1993) and the jump-diffusion model of Merton (1976). For both these models, we analyze which parameters are most important to match certain stylized empirical facts. The main difference between SV and SJ is the term structure of the smile. While the smile flattens out for longer times to maturity in both cases, the impact of the time to maturity is much stronger in an SJ model than in an SV model. This is also pointed out by Das and Sundaram (1999) and Carr and Wu (2003), who both compare SV and SJ models.

Second, we analyze more general models. Bakshi, Cao, and Chen (1997) and Bates (1996) propose models with both SV and SJ. Bates (2000) introduces a model which includes stochastic jumps and two stochastic volatility processes (instead of only one). We interpret these models as combinations of SV and SJ models, which allows us to rely on the detailed discussion of the impact of the parameters in these basic models. We can thus focus exclusively on the effect that the combination of several risk factors has on the smile. What characteristics of the smile can be explained in the combined models, but not in the basic models? The structure of our analysis emphasizes that these additional characteristics of more sophisticated models are not primarily generated by the pure inclusion of SV or SJ, but are achieved by a clever combination of the two.

The results of this analysis turn out to be highly relevant for the choice of a pricing model. While the use of a complex model seems preferable at first sight, it also comes at a cost. The complex model is harder to implement, and its many more parameters are more difficult to estimate. This motivates the use of a model that is as parsimonious as possible. Given a certain model, one should switch to a more general model only if the latter offers a significant improvement relative to the given model, in that it fits the prices better or improves the performance of hedging strategies. Assume, e.g., that the only information available is a cross section of European option prices and that we have found a model that can explain this cross section. Then, the use of a more complicated model is hard to justify, in particular since it would include additional parameters that could not be identified from the given cross section of option prices anyway.

The model of Bakshi, Cao, and Chen (1997) combines SV and SJ. The relative weight of these two components determines the term structure of implied volatilities. The larger the weight of stochastic jumps, the faster the smile becomes flat with increasing time

to maturity, and the steeper the smile for very short times to maturity. The model thus allows for a better fit of smiles for different times to maturity. Bates (2000) combines SJ with two processes for SV. We omit the jump-component here and focus on the two-factor SV model. The use of two factors instead of one results in a stochastic correlation of stock returns and variance. The skewness of the smile is then also stochastic, and depending on the parameterisation, we can observe both an upward and a downward sloping smile over time. This is particularly important for currency options, as argued by Carr and Wu (2004). They propose a model with two Lévy processes and a stochastic time change to capture the stochastic skew, whereas our analysis shows that the same result can be achieved with two standard square-root diffusions for the stochastic return variance. One component implies a positive, the other one a negative skewness, and the respective weights are stochastic.

The paper is organised as follows. In Section 2 we give a short overview of the main pricing techniques and discuss the link between the moments of the risk-neutral distribution and the shape of the smile. The two basic models of Heston (1993) and Merton (1976) are discussed in Section 3, and combinations of these models are analysed in Section 4. Section 5 concludes.

2 Pricing, Volatility Smile, and Risk-Neutral Moments

2.1 Pricing

There are several approaches to price contingent claims. We start with the risk-neutral pricing equation. Since prices normalized by the money-market account are martingales under the risk-neutral measure Q, we can calculate the price C_t for a European claim with terminal payoff C_T as

$$C_t \;=\; E^Q\left[e^{-\int_t^T r_v dv} C_T \mid \mathcal{F}_t\right] \tag{1}$$

where r_v is the risk-free rate at time v. We do not discuss how to determine the risk-neutral measure here, i.e. we do not deal with problems that arise in an incomplete market where not all market prices of risk are known. Furthermore, we assume in the following that the interest rate is constant and equal to r. A stochastic interest rate has only a minor impact on the prices of European options, and most empirical studies also use a deterministic interest rate.

If the price of a European claim C can be written as a function of the state variables, e.g. $C_t = c(t, S_t, V_t, \ldots)$ in an SV model where S denotes the stock price and V is the local variance, then the function c has to satisfy a partial differential equation. The exact form of this partial differential equation depends on the model under consideration, and we will give it for each of the models discussed below. The formal relationship between this partial differential equation and the risk-neutral pricing formula (1) is provided by the Feynman-Kac theorem. More details can be found in Bingham and Kiesel (1998) or Duffie (2001).

To calculate the price via the risk-neutral pricing formula (1), one has to know the risk-neutral distribution. In the model of BS, the risk-neutral density is log-normal, and the expectation of the normalized call payoff can easily be calculated. In more sophisticated models like Heston (1993) or Bakshi, Cao, and Chen (1997), there is no closed form solution for the risk-neutral density. One can then use Monte Carlo simulation to evaluate the expectation. An alternative approach is to rely on characteristic functions. This technique is used in Heston (1993), and it is formalized and put into a more general framework by Bakshi and Madan (2000) and Duffie, Pan, and Singleton (2000). The main task is to determine the Fourier transform of the state price density

$$\phi(u, t, T, S_t, \ldots) \;=\; E^Q\left[e^{-\int_t^T r_v dv} e^{iu \ln S_T} \mid \mathcal{F}_t\right]. \tag{2}$$

The risk-neutral density of the stock price and the price of a call option can then be calculated by Fourier inversion. The price of a European call on the stock with strike price K is

$$C_t \;=\; S_t \Pi_1 - K B_t(T) \Pi_2, \tag{3}$$

where

$$\begin{aligned}
\Pi_1 &= \frac{1}{2} + \frac{1}{\pi}\int_0^\infty \Re\left[\frac{\phi(u - i, t, T, S_t, \ldots) e^{-iu \ln K}}{iuS_t}\right] du \\
\Pi_2 &= \frac{1}{2} + \frac{1}{\pi}\int_0^\infty \Re\left[\frac{\phi(u, t, T, S_t, \ldots) e^{-iu \ln K}}{iuB_t(T)}\right] du \\
B_t(T) &= E^Q\left[e^{-\int_0^T r_v dv} \mid \mathcal{F}_t\right]
\end{aligned}$$

and where $\Re$ denotes the real part of a complex number. Instead of a simulation of a large number of paths this approach involves a (much faster) numerical integration. Of course, this technique hinges on the ability to determine the Fourier transform (2). For affine jump diffusions, the general approach can for example be found in Duffie, Pan, and Singleton (2000).

2.2 Moments of the Risk-Neutral Distribution and Their Impact on Option Prices

In the following sections, we will discuss the impact of the model choice and of the parameters on the implied volatility smile. It turns out that in this context the moments of the risk-neutral distribution play an important role. We will therefore often proceed in two steps, in that we first analyze the impact of the parameters and the model choice on the moments of the risk-neutral distribution and then consider the impact of these moments on the smile. We focus on variance, skewness and kurtosis, since the mean of the risk-neutral distribution is fixed by the current price of the stock. This can be seen from the risk-neutral pricing equation

$$S_0 \;=\; E^Q\left[e^{-rT}S_T\right]$$

where we have assumed a deterministic interest rate.

Assume that the variance increases while the mean remains constant. The distribution is then wider, and probability mass is shifted from returns close to the center of the distribution to returns further in the tails. So, for basically all options along the strike price axis, the probability of a positive payoff increases, which leads to a higher overall level of the smile curve.

The skewness determines the relation between the prices of out-of-the money (OTM) puts and OTM calls. We assume that the mean and the variance of the stock price under the risk neutral measure remain constant, that is the expectations of S and S^2 under the risk-neutral measure are fixed. Given our assumption of deterministic interest rates, this implies that the prices of the stock S and the quadratic payoff S^2 are fixed. If skewness decreases, probability mass is shifted from very high stock prices to very low stock prices. The prices of OTM calls, which pay off for high stock prices, thus decrease, and the prices of OTM puts, which have a payoff for low stock prices, increase. For a negative skewness, we therefore expect the implied volatility (IV) of OTM puts to be larger than the IV of OTM calls, so that we see a downward sloping smile. Our notation is a bit loose here, since the term 'downward sloping smile' does not imply a monotonicity of the implied volatility function in a rigorous mathematical sense.

Bates (1997) defines a skewness premium where he compares the price of an OTM call to the price of an OTM put for strikes with a geometric average equal to the current

forward price of the underlying. For $x > 0$, the skewness measure is

$$SK_t(x) = \frac{C(t, S_t, S_t e^{r(T-t)}(1+x), \ldots)}{P(t, S_t, S_t e^{r(T-t)}(1+x)^{-1}, \ldots)} - (1+x). \quad (4)$$

This skewness measure is zero in the model of BS. If it is negative, the IV of OTM puts is larger than the IV of OTM calls, and the smile is downward sloping.

The kurtosis determines the curvature of the smile. We assume that the mean, the variance and the skewness of the distribution are given, so that, analogous to the discussion above, the prices of the stock S, the quadratic payoff S^2 and the cubic payoff S^3 are fixed. If the kurtosis increases, there is more probability mass in the tails of the distribution, so very low and very high stock prices both have a higher probability. This increases the prices of OTM puts and OTM calls. At the same time, the price of the quadratic payoff remains constant. It can be replicated by a static portfolio of long positions in a continuum of calls with strike prices going from zero to infinity, where we use that

$$S_T^2 = \int_0^\infty 2(S_T - K)^+ dK$$

which implies

$$E^Q\left[e^{-rT} S_T^2\right] = 2\int_0^\infty C(0, S_0, K, T, \ldots) dK.$$

A proof is e.g. given in Carr and Madan (2001). For the price of this portfolio to remain constant, some call options must have a lower price, and it can be argued that these will be ATM. An increase in the kurtosis thus tends to increase the IV of OTM options and to decrease the IV of ATM options. Thus, the curvature of the smile increases, and the smile gets more pronounced.

To sum up the main arguments: In the model of BS, the smile is flat. The stock price follows a log-normal distribution, the stock return is normally distributed. If the skewness of the risk-neutral distribution is lower than in the model of BS, we expect to see a downward sloping smile. If the kurtosis of the risk-neutral distribution is larger than for BS, we expect to see a smile where the IV of OTM options is larger than the IV of ATM options.

3 Stochastic Volatility and Jump-Diffusion Models

When it comes to option pricing, stochastic volatility and stochastic jumps are the main risk factors besides stock price risk. Most option pricing models assume that at least one

of these additional risk factors is present or combine both of them. In this section, we provide a detailed analysis of the two most prominent models that include either stochastic volatility or stochastic jumps, the models of Heston (1993) and Merton (1976). We want to see how the smile depends on the parameters of the models, and we also focus on the differences between the two risk factors. In the analysis of more sophisticated models in Section 4, we take the results on the impact of the parameters as given, and focus on the additional effects of combining several risk factors. It will turn out that this approach allows for a nicely structured analysis of the models.

3.1 Stochastic Volatility Models

Heston (1993) assumes that the local variance V of the stock follows a square root process, that is a mean-reverting process whose volatility is proportional to the square root of V. This process is sometimes also called a CIR-process, since it is used in the model of Cox, Ingersoll, and Ross (1985) to describe the dynamics of the short term interest rate. The Heston model allows for a non-zero correlation between changes in the local variance and in the stock price.

The stochastic differential equations (sde) for the stock price S and the local variance V under the risk-neutral measure Q are

$$\begin{aligned} dS_t &= rS_t dt + \sqrt{V_t} S_t d\widetilde{W}_t^S \\ dV_t &= \kappa(\theta - V_t)dt + \sigma_V \sqrt{V_t}\left(\rho d\widetilde{W}_t^S + \sqrt{1-\rho^2} d\widetilde{W}_t^V\right), \end{aligned}$$

where $\widetilde{W}^S$ and $\widetilde{W}^V$ are two uncorrelated Wiener processes. The local variance follows a mean-reversion process with mean-reversion level θ and mean-reversion speed κ, and its uncertainty is governed by the 'volatility of volatility' σ_V. The correlation between the stock price and the local variance is ρ. For most stock and index options, this correlation is estimated to be negative which is also referred to as the leverage effect.

The pricing of contingent claims can be done by solving the fundamental partial differential equation or by calculating the risk-neutral expectation either by Monte-Carlo simulation or by Fourier inversion. The exact form of the partial differential equation and of the Fourier transform (2) are given in Appendix A.1. If $\rho = 0$, that is if stock returns and the local variance are uncorrelated, the price of a European call option can also be calculated as an average over BS prices, as shown in Hull and White (1987).

In the model of BS, the log return of the stock follows a normal distribution with zero skewness and zero excess kurtosis. A stochastic volatility model can generate both

skewness and positive excess kurtosis. The correlation between volatility and stock prices results in a positive or negative skewness of the risk-neutral distribution, depending on the sign of the correlation, so that the smile can be upward or downward sloping. Furthermore, stochastic volatility increases the excess kurtosis of the distribution and thus can explain a smile where the IV of OTM options is larger than the IV of ATM options.

To gain some intuition for the SV model, we first consider the local variance V_t of the stock return. Its conditional expectation is equal to

$$E^Q[V_u|\mathcal{F}_t] \;=\; e^{-\kappa(u-t)}V_t + \left(1 - e^{-\kappa(u-t)}\right)\theta,$$

and it represents a weighted average of the current level V and the long run mean θ. The larger the speed of mean reversion κ, the larger the weight of the long-run mean. The expected realized variance over the time interval $[t, T]$ is

$$E^Q\left[\frac{1}{T-t}\int_t^T V_u du \;\Big|\; \mathcal{F}_t\right] \;=\; \theta + \frac{1 - e^{-\kappa(T-t)}}{\kappa(T-t)}\,(V_t - \theta), \tag{5}$$

so it also represents a weighted average of the current local variance and the long-run mean. Note that both expectations depend neither on the volatility of volatility nor on the correlation.

Das and Sundaram (1999) also calculate higher conditional moments of the log stock returns. They show that the skewness of the risk-neutral distribution is negative if and only if ρ is negative, and that it goes to zero for very short and very long time intervals. Furthermore, they show that excess kurtosis is always positive, and that it also goes to zero for very short and very long maturities.

For the following numerical examples, we rely on parameters very close to the estimates in Bates (2000). The parameters are $\kappa = 1.5$, $\theta = 0.25^2$, $\sigma_V = 0.75$, $\rho = -0.5$, and we assume that V_0 is equal to its long-run mean θ. The interest rate is set to zero, so that the strike price of an ATM option is always equal to the current stock price, which facilitates the comparison of the smile curves for different times to maturity. This base case gives rise to a mostly downward sloping volatility smile with a slightly increasing part for OTM calls.

The impact of ρ is shown in Figure 1. For a negative ρ, the risk-neutral distribution of the stock returns is left-skewed, so that the smile is downward sloping, and vice versa. A change in ρ thus rotates the smile: if ρ decreases, the IV of OTM puts increases, while the IV of OTM calls decreases. In the special case where $\rho = 0$, the risk-neutral distribution has zero skewness. The smile is symmetric, and the skewness premium (4) is zero. A proof

of this statement is given in Bates (1997). For the following analysis, we assume a negative correlation ρ.

The time to maturity also has an impact on the smile. For very long maturities, the smile becomes flat, and the implied volatilities converge to the long-run mean. However, this convergence is not necessarily monotonic. A more detailed discussion of this issue will be provided in Section 3.2, where we compare the term structure of implied volatilities in the SV model and in the jump-diffusion model.

The overall level of implied volatilities depends mainly on the local variance V and on its long run mean θ. The higher either V or θ, the greater the implied volatilities. A formal proof can be constructed along the lines of Henderson, Hobson, Howison, and Kluge (2004). To get the intuition, note that the expected realized variance (5) is an increasing function of both V and θ, so we expect also the overall level of the smile to increase in V and θ. Figure 2 shows the impact of V (upper row) and of θ (lower row) for different times to maturity. A comparison of the graphs shows that V has more impact on the IV for short times to maturity, while the influence of θ is more important for longer-term options. This can be explained by noting that the local variance follows a mean-reverting process. For long times to maturity, the current value V_t is much less important than the mean-reversion level. For short times to maturity, on the other hand, there is not much time for V to be pulled back towards its long run mean, so that the current value of the local variance V is more important.

The curvature of the smile mainly depends on the mean-reversion speed κ and on the volatility of volatility σ_V. Both these parameters have an impact on the variation of the local variance V. The larger this variation, the larger the kurtosis of the risk-neutral distribution, and the more pronounced the smile. Since the variation of V increases with increasing volatility of volatility σ_V, the smile is the steeper the larger σ_V. On the other hand, an increase in κ implies that the local variance V is pulled back to its long run mean faster, which reduces the variation of V, and thus results in a flatter smile. Figure 3 shows that the impact of the two parameters σ_V and κ differs across different times to maturity. While the volatility of volatility has a similar impact on the smile for all times to maturity, the mean-reversion speed κ has more impact for medium and long times to maturity. To explain the latter finding, note that κ determines how fast V reverts to its long run mean. The larger κ, the faster V is pulled back, and the faster the smile thus dies out.

Figure 4 shows that the impact of κ is different for different values of V, while the

impact of σ_V is again approximately the same for all values of V. Implied volatilities are increasing in κ if the current volatility is well below its long run mean, and vice versa. This can again be explained by the fact that variance follows a mean-reversion process. If the current value of V is below its long run mean, the reversion to θ is the faster the higher κ, and we expect V to increase more until the maturity of the option. A higher κ thus increases the expected realized variance (5), and the overall level of the smile increases. The argument for $V \gg \theta$ is exactly analogous.

Finally, we consider a scaling of the diffusion component, i.e. we assume that the diffusion component of the stock is multiplied by some scaling factor α. This will be important for the analysis of combined models in Section 4 where we will mainly be interested in the impact that the weights of the diffusion and jump component have on the form of the smile and where a change in the weight of stochastic volatility will amount to a scaling of SV. The scaling of the diffusion component can be interpreted as replacing $\sqrt{V}$ by $\sqrt{\widetilde{V}} = \alpha\sqrt{V}$. The process for the new, scaled variance $\widetilde{V}$ is then given by

$$d\widetilde{V}_t \;=\; \kappa(\alpha^2\theta - \widetilde{V}_t)dt + \alpha\sigma_V\sqrt{\widetilde{V}_t}dW_t.$$

Figure 5 shows the impact of α on the volatility smile. It can be seen that, as expected, the overall level of implied volatilities is increasing in α. Furthermore, this holds for all times to maturity, whereas a change in either V or θ mainly had an impact for short or for long times to maturity. And finally, the form of the smile remains approximately the same, while the change of V or θ also changed the form of the smile as can be seen from Figure 2.

3.2 Jump-Diffusion Models

The most prominent SJ model is the jump-diffusion model of Merton (1976). The sde for the stock price under the risk-neutral measure Q is

$$dS_t \;=\; \left(r - E^Q[e^{X_t} - 1]\lambda_0\right) S_t dt + \sigma S_t d\widetilde{W}_t + \left(e^{X_t} - 1\right) S_{t-} dN_t$$

where N is a Poisson process with intensity λ_0. The jump size X in log returns is stochastic and follows a normal distribution:

$$X_t \sim N\left(\ln(1+\mu_X) - 0.5\sigma_X^2, \sigma_X^2\right).$$

We assume that the distribution of X neither depends on time t nor on the state variables of the model. Furthermore, N and $\widetilde{W}$ are assumed to be independent.

The exact form of the partial differential equation and of the Fourier transform (2) are given in Appendix A.2. In the model of Merton (1976), the price of a European call option can also be calculated as an average over BS prices. To derive this result, one uses the observation that conditional on the number of jumps, the stock price at time T follows a log-normal distribution, so that the conditional price of the European option is just a BS price. Taking the expectation over these prices with respect to the number of jumps yields the price of the option in the jump-diffusion model.

If only the stock and the money market account are traded, the model is incomplete. While in the SV model of Heston (1993) one additional non-affine claim is enough to complete the market, the number of additional instruments needed in an SJ model is equal to the number of possible jump sizes. If these jumps are, like in the model of Merton (1976), drawn out of a continuous distribution, we need a continuum of claims to complete the market.

Like a stochastic volatility model, a jump-diffusion model can generate a skewed risk-neutral distribution with excess kurtosis. We now first consider the higher moments of the log return of the stock, which were calculated by Das and Sundaram (1999). The local variance of the stock return is

$$\sigma^2 + \lambda_0 E^Q[X^2] \;=\; \sigma^2 + \lambda_0 \left[\sigma_X^2 + \left(\log(1+\mu_X) - 0.5\sigma_X^2\right)^2\right]. \tag{6}$$

The relative weight of the jump component is called the jumpiness, and in the following, we will also be interested in its impact on the smile. The skewness of the return is

$$\frac{\lambda_0 E^Q[X^3]}{\left(\sigma^2 + \lambda_0 E^Q[X^2]\right)^{1.5}\sqrt{\tau}}.$$

It is inversely proportional to the square root of the time to maturity τ. The kurtosis of the return is

$$3 + \frac{\lambda_0 E^Q[X^4]}{\left(\sigma^2 + \lambda_0 E^Q[X^2]\right)^2 \tau},$$

so that the excess kurtosis is always positive and proportional to the inverse of the time to maturity. Both skewness and excess kurtosis thus decrease with increasing time to maturity. In contrast to the SV model, they do not go to zero for a very short time to maturity.

The numerical examples use a base case where we have chosen the parameters such that we see a pronounced smile for options with a time to maturity of six months, and such that the jumpiness of the stock return is equal to 50%. The parameters we use are $\sigma = 0.18$, $\lambda_0 = 0.897556$, $\mu_X = -0.1$, and $\sigma_X = 0.15$.

Figure 6 compares the impact of the time to maturity in the models of Merton (1976) and Heston (1993). The model of Heston (1993) is calibrated to the prices of European options as calculated in the model of Merton (1976) with six months to maturity and with strike prices between 90 and 110. The relative pricing errors for these options are below 0.3%. It can be seen from the graphs that in both models the smile is flattening out for long maturities. However, the remaining life of the option has much more impact on the smile in the jump-diffusion model than in the SV model. For a time to maturity of six months, the smiles coincide by construction. If the time to maturity increases, then in the jump-diffusion model the smile flattens out faster than in the SV model. If the time to maturity decreases, the differences between the models are even greater. The smile in the stochastic volatility becomes only slightly steeper, while in the jump-diffusion model, it is a lot steeper for one month than for six months. If we want to obtain large differences in the smile for different times to maturity and a very steep smile for short times to maturity, the jump-diffusion model is thus better than the SV model.

The intuitive reason for the significantly different impact of the time to maturity in the SV and the SJ model can be found by looking at the skewness and kurtosis of the risk-neutral distribution. In the jump-diffusion model, both moments decrease monotonically with increasing time to maturity and ultimately go to zero for very long time to maturity. The smile thus flattens out with increasing time to maturity. In the SV model, skewness and excess kurtosis go to zero for very long and also for very short times to maturity. For short to moderate times to maturity, however, they even increase. This increase slows down the flattening out of the smile.

Besides the impact of the time to maturity on the form of the smile, one may also consider the term structure of the IV of ATM options. For $\rho = 0$ in the SV model, and for $E^Q[X] = 0$ in the SJ model, the IV of an ATM option is approximately equal to the expected realized variance of the return over the time to maturity. Furthermore, Merton (1976) shows that in a jump-diffusion model, the IV of an ATM option is increasing in time to maturity. On the other hand, it may be an increasing, decreasing or even hump-shaped function of time to maturity in an SV model. More details are given in Hull and White (1987) and Das and Sundaram (1999).

The skewness of the smile depends on the sign of the expected jumps $E^Q[X]$ in log returns. This can also be seen in Figure 7. If μ_X is negative, the smile is downward sloping, and the IV of OTM puts is higher than the IV of OTM calls. In this case, jumps mainly reduce the stock price, and probability mass is shifted from high stock prices to low

stock prices. The risk-neutral distribution is thus more left-skewed than the log-normal distribution. For $\mu_X > 0$ and for $\mu_X = 0$, the line of argument is completely analogous, showing that the smile is upward sloping and flat, respectively. In the following, we assume $\mu_X < 0$.

The parameters σ, λ_0 and σ_X all increase the level of implied volatilities, as can be seen in Figure 8. This can easily be explained by the fact that the variance (6) of stock returns is increasing in these parameters.

The curvature of the smile depends on the kurtosis of the risk-neutral distribution. It can be seen from Figure 8 that the smile is the more pronounced the higher σ_X, since excess kurtosis is increasing in this parameter. For $\sigma_X = 0$, the smile is a monotone function of the strike price, and if σ_X increases, we start to see a true smile, where the IV of both OTM calls and puts is larger than the IV of ATM calls. This implies that for an increase of σ_X, the IV of OTM options increases more than the IV of ATM options. Furthermore the smile is the flatter the larger the volatility of the diffusion component. To get the intuition, note that the part of the variance explained by jumps, is the smaller the larger this diffusion volatility. A smaller jumpiness leads to a lower skewness and excess kurtosis, and the smile becomes flatter. So σ has a more pronounced impact on the IV of ATM options.

In the SV model, we have discussed how to scale the volatility to adjust the variance of the stock to some given level. We now repeat this analysis in the model of Merton (1976). Assume that the total variance (6) is multiplied by α^2, and that jumpiness stays constant. For the diffusion component, this implies that σ is replaced by $\widetilde{\sigma} = \alpha\sigma$. For the jump component, we could vary the intensity, or the jump size, or both. To keep the effects of changes in λ_0 and X separated, we only consider their independent variation. So λ_0 would be replaced by $\widetilde{\lambda}_0 = \alpha^2\lambda_0$, and the new jump size would be $\widetilde{X} = \alpha X$. The new distribution of jump size $\widetilde{X}$ will then be

$$\widetilde{X} \;\sim\; N\left(\ln(1+\widetilde{\mu}_X) - 0.5\widetilde{\sigma}_X^2, \widetilde{\sigma}_X^2\right),$$

with parameters

$$\begin{aligned}\widetilde{\mu}_X &= \exp\left\{\alpha\ln(1+\mu_X) + 0.5\sigma_X^2(\alpha^2-\alpha)\right\} - 1\\ \widetilde{\sigma}_X &= \alpha\sigma_X.\end{aligned}$$

It can be easily checked that the jumpiness indeed remains constant. Figure 9 shows the effect of the above changes on the smile. The graphs confirm that the overall level of

implied volatilities is indeed increasing in the scaling factor. They also show that the impact on the shape of the smile is stronger for an adjustment of the jump intensity than for an adjustment of the jump size. To get the intuition, consider the formulas for skewness and excess kurtosis. They show that a change in the jump size does not change skewness and kurtosis, whereas for a change in jump intensity, both skewness and kurtosis are decreasing functions of the scaling parameter α. If the jump intensity is adjusted, the shape of the smile is thus changing, and it becomes the flatter the larger the scaling parameter.

These results show that the decomposition of the jump component is important for the shape of the smile. To analyze this impact in more detail, we fix the total variance and the jumpiness at some level. Then, we change two out of the three jump parameters λ_0, σ_X and μ_X such that the contribution of the jump component to the total variance of returns remains constant. First, assume that we start from a negative μ_X and decrease it further, that is we make jumps even more negative. The risk-neutral distribution becomes more left-skewed, which results in a twist of the IV-function in that the IV of OTM puts increases and the IV of OTM calls decreases. At the same time, however, total variance has increased, and this has to be offset by reducing either the volatility of jumps or the jump intensity. If jump volatility is reduced, then the excess kurtosis of the distribution is reduced, which makes the smile flatter. If jump intensity is reduced, the curvature of the smile is not affected significantly. Second, assume that an increase in σ_X goes together with a decrease in λ_0. The main effect of this change is an increase in kurtosis which makes the smile more pronounced.

As the last point, we analyze the impact of the jumpiness. The jump-diffusion model can be interpreted as a mixture of a pure jump model without any diffusion component and the model of BS without any jumps. The question is then which impact the weights of these two components have on the smile. The two extremes are given by a jumpiness of zero, where the smile is flat, and a jumpiness of one, where the smile has maximum curvature. The larger the jumpiness, the steeper the smile is, as can be seen from Figure 10. It furthermore compares two ways to deal with jumps when their contribution to total variance changes. Either the jump intensity or the jump size can be adjusted, as discussed above for the case of scaling the total variance. An adjustment of the jump size has a larger impact on the skewness and kurtosis, and thus also on the form of the smile, than an adjustment of the jump intensity.

4 Models With Several Risk Factors

Most models discussed in the literature are more sophisticated than the basic approaches presented in the last section. To justify the use of a more complicated model, one has to show that there are significant differences in pricing or hedging and that the more general models can explain stylized facts about option prices not explained by the basic models. We focus on pricing differences and interpret the more complex models as combinations of the respective basic models. Given our discussion in Section 3, we can focus exclusively on the effect of combining several risk factors.

4.1 SVJ Model: Bakshi, Cao, and Chen (1997)

The model of Bakshi, Cao, and Chen (1997) combines stochastic volatility, stochastic jumps, and even stochastic interest rates. We consider a simplified version with deterministic interest rates, since the impact of interest rate risk on the prices of European options is rather small. The setup of this SVJ model under the risk-neutral measure Q is

$$\begin{aligned} dS_t &= \left(r - E^Q[e^{X_t} - 1]\lambda_0\right) S_t dt + \sqrt{V_t} S_t d\widetilde{W}_t^S + \left(e^{X_t} - 1\right) S_{t-} dN_t \\ dV_t &= \kappa(\theta - V_t)dt + \sigma_V \sqrt{V_t}\left(\rho d\widetilde{W}_t^S + \sqrt{1-\rho^2} d\widetilde{W}_t^V\right), \end{aligned} \tag{7}$$

where N is a Poisson process with intensity λ_0. Like in the model of Merton (1976), the jump size in the log returns follows a normal distribution:

$$X_t \sim N\left(\ln(1+\mu_X) - 0.5\sigma_X^2, \sigma_X^2\right).$$

Furthermore, we assume that the distribution of the jump size neither depends on time nor on other state variables. The interpretation of the process for stochastic volatility is the same as in the model of Heston (1993) discussed in Section 3.1. The fundamental partial differential equation and the Fourier transform (2) for this model are given in Appendix A.3. Setting $\lambda_0 = 0$ yields Heston's pure SV model, while choosing $\sigma_V = 0$ together with $V_0 = \theta = \sigma^2$ results in Merton's jump-diffusion model.

The local variance of the stock return is

$$V_t + \lambda_0 E^Q[X^2] = V_t + \lambda_0\left((\log(1+\mu_X) - 0.5\sigma_X^2)^2 + \sigma_X^2\right).$$

Like in the model of Merton (1976), we define the jumpiness as the relative contribution of the jump component to the local variance.

The numerical examples are based on the parameter estimates of Bakshi, Cao, and Chen (1997), where we have adjusted the jump parameters such that jumps are more pronounced and that the jumpiness is equal to 0.5 when the local variance coincides with its long run mean. The parameters are

$$\theta = \frac{0.04}{2.03},\ \kappa = 2.03,\ \sigma_V = 0.38,\ \rho = -0.57,\ \lambda_0 = 1.1925,\ \mu_X = -0.10,\ \sigma_X = 0.07,$$

and the local variance V is set equal to its long run mean θ.

The impact of the parameters of the stochastic volatility process and of the jump component had already been analyzed in detail in Section 3. This allows us to focus exclusively on the characteristics of the smile that are due to a mixture of these two components and to analyze the impact of the jumpiness. We start from a total local variance Y_0. For a jumpiness of α, the jumps contribute αY_0 while the share of the diffusion component is $(1-\alpha)Y_0$, both measured as of time $t = 0$. When we change the jumpiness, we thus have to adjust the diffusion component and the jump component to these contributions. This scaling is done like in Section 3. For SV, the local variance V_t is replaced by

$$\widetilde{V}_t = \frac{(1-\alpha)Y_0}{V_0} V_t.$$

For SJ, we again consider two possibilities. We can either replace the jump intensity λ_0 by

$$\widetilde{\lambda}_0 = \frac{\alpha Y_0}{\lambda_0 E^Q[X^2]} \lambda_0,$$

or we can replace the jump size X by

$$\widetilde{X} = \sqrt{\frac{\alpha Y_0}{\lambda_0 E^Q[X^2]}}\ X.$$

Figure 11 shows the impact of the jumpiness on the smile. For a jumpiness of zero, only stochastic volatility is remaining, while for a jumpiness of one, we have a pure jump process. In both cases, there is a smile, and for our parametrization, which represents a quite common scenario, this smile is downward sloping. In Section 3.2, we had seen that the main difference between stochastic volatility and stochastic jumps is that the smile for a jump model is much more pronounced for short maturities, and it dies out much faster for increasing time to maturity. The larger the weight of the jump, the more the smile in the model of Bakshi, Cao, and Chen (1997) inherits this behavior. Again, the main difference between the two possibilities to scale the jump component is that a scaling of the jump size has a larger impact on the form of the smile than a scaling of the jump intensity.

4.2 SVJ Model With Volatility-Dependent Jump Intensity

A slight modification of the model of Bakshi, Cao, and Chen (1997) is given by a model where the jump intensity is not a constant, but proportional to local variance V. This represents a simplification of Bates (2000), with a model setup under the risk-neutral measure Q given by

$$\begin{aligned} dS_t &= \left(r - E^Q[e^X - 1]\lambda_1 V_t\right) S_t dt + \sqrt{V_t} S_t d\widetilde{W}_t^S + \left(e^{X_t} - 1\right) S_{t-} dN_t \\ dV_t &= \kappa(\theta - V_t)dt + \sigma_V \sqrt{V_t}\left(\rho d\widetilde{W}_t^S + \sqrt{1-\rho^2} d\widetilde{W}_t^V\right). \end{aligned} \tag{8}$$

The intensity of the Poisson process N is now given by $\lambda_1 V_t$, and the jump-size X in returns is again normally distributed:

$$X_t \sim N\left(\ln(1+\mu_X) - 0.5\sigma_X^2, \sigma_X^2\right).$$

The fundamental partial differential equation and the Fourier transform (2) for this model are given in Appendix A.4.

The total local variance of the stock return is

$$V_t + \lambda_1 V_t E^Q[X_t^2] = V_t + \lambda_1 V_t \left((\log(1+\mu_X) - 0.5\sigma_X^2)^2 + \sigma_X^2\right). \tag{9}$$

A calculation of the jumpiness shows that it is a constant, whereas in the model of Bakshi, Cao, and Chen (1997), the jumpiness is a decreasing function of the stochastic variance V. The fact that the jumpiness can be held constant is often mentioned as one of the key advantages of a model like (8) with a variance-dependent jump intensity.

To compare the model of Bakshi, Cao, and Chen (1997) to the setup in (8), we use the parameters from Section 4.1 and set $\lambda_1 = \lambda_0/\theta$, so that the jump intensity in both models coincides for a local variance equal to its long run mean θ. A first inspection shows that the impact of V on the level of implied volatilities is larger for a volatility-dependent jump intensity than for a constant intensity. To get the intuition behind this result, note that in model (8) a change in the local variance V has a larger impact on the total local variance than in the BCC model. This results in a larger impact of V on the overall level of the smile. Second, the smile in model (8) is steeper than in the BCC model. The intuitive reason is that the additional variation introduced into the jump intensity increases the kurtosis of the distribution, so that the smile is steeper.

4.3 Two-Factor Stochastic Volatility Models

As the last model, we consider a simplified version of Bates (2000) where we omit the jump component. In this model, there are two processes for stochastic volatility instead of only one. The model specification under the risk-neutral measure Q is given by

$$\begin{aligned} dS_t &= rS_t dt + \sqrt{V_t^{(1)}} S_t d\widetilde{W}_t^{1,S} + \sqrt{V_t^{(2)}} S_t d\widetilde{W}_t^{2,S} \\ dV_t^{(1)} &= \kappa^{(1)} \left(\theta^{(1)} - V_t^{(1)}\right) dt + \sigma_V^{(1)} \sqrt{V_t^{(1)}} \left(\rho^{(1)} d\widetilde{W}_t^{1,S} + \sqrt{1-(\rho^{(1)})^2} d\widetilde{W}_t^{1,V}\right) \\ dV_t^{(2)} &= \kappa^{(2)} \left(\theta^{(2)} - V_t^{(2)}\right) dt + \sigma_V^{(2)} \sqrt{V_t^{(2)}} \left(\rho^{(2)} d\widetilde{W}_t^{2,S} + \sqrt{1-(\rho^{(2)})^2} d\widetilde{W}_t^{2,V}\right) \end{aligned} \tag{10}$$

The Wiener processes $\widetilde{W}^{1,S}$, $\widetilde{W}^{2,S}$, $\widetilde{W}^{1,V}$, and $\widetilde{W}^{2,V}$ are independent. The parameters of the two stochastic volatility processes coincide with the parameters in the model of Heston (1993) and were already discussed in Section 3.1. The total local variance of the stock is equal to $V_t = V_t^{(1)} + V_t^{(2)}$. Further details of this specification, in particular the correlation between the stock returns and the total local variance, will be discussed below. The fundamental partial differential equation and the Fourier transform (2) for this model are given in Appendix A.5.

The two-factor model (10) nests the model of Heston (1993). To see this, assume that the parameters of the model of Heston (1993) and the local variance V are given. Then we specify the two-factor model (10) such that $\kappa^{(i)} = \kappa$, $\sigma_V^{(i)} = \sigma_V$, $\rho^{(i)} = \rho$, for $i = 1, 2$, and we choose the current local variances and their long run means such that $V = V^{(1)} + V^{(2)}$ and $\theta^{(1)} + \theta^{(2)} = \theta$. A straightforward calculation shows that the local variance $V^{(1)} + V^{(2)}$ follows the desired square-root process, and that the correlation between stock returns and local variance is equal to ρ.

In the following, we take the model of Heston (1993) as a benchmark and discuss which innovations are provided by using two stochastic volatility factors. It is clear from the analysis in the previous paragraph that the two-factor model will only differ from the one-factor model if the two volatility processes have different correlations with stock returns, different volatilities of volatility, or different speeds of mean reversion. We focus on the differences in the correlations, since these allow for a stochastic skew, which cannot be explained in any of the other models discussed so far in this paper.

The main point to note is that in the two-factor model, both the volatility of volatility and the correlation between stochastic volatility and stock returns are stochastic. To see this, take a closer look at the total local variance of the stock return given by

$$V_t = V_t^{(1)} + V_t^{(2)}.$$

Its long run mean is equal to $\theta^{(1)} + \theta^{(2)}$, and the local volatility of volatility is

$$\sqrt{\frac{V_t^{(1)}}{V_t^{(1)} + V_t^{(2)}} \left(\sigma_V^{(1)}\right)^2 + \frac{V_t^{(2)}}{V_t^{(1)} + V_t^{(2)}} \left(\sigma_V^{(2)}\right)^2}.$$

It is a weighted average of the local volatilities of the two stochastic volatility processes, and the larger the contribution of $V^{(1)}$ to the local variance, the more the local volatility of volatility is shifted towards $\sigma_V^{(1)}$.

The local correlation between the stock price and the local variance is

$$\frac{\frac{V_t^{(1)}}{V_t^{(1)}+V_t^{(2)}} \sigma_V^{(1)} \rho^{(1)} + \frac{V_t^{(2)}}{V_t^{(1)}+V_t^{(2)}} \sigma_V^{(2)} \rho^{(2)}}{\sqrt{\frac{V_t^{(1)}}{V_t^{(1)}+V_t^{(2)}} \left(\sigma_V^{(1)}\right)^2 + \frac{V_t^{(2)}}{V_t^{(1)}+V_t^{(2)}} \left(\sigma_V^{(2)}\right)^2}},$$

which depends on the current realizations of $V^{(1)}$ and $V^{(2)}$. If $\rho^{(1)}$ and $\rho^{(2)}$ have different signs, the local correlation can be positive or negative, and depending on the current local volatilities, we will either see an upward or a downward sloping smile. The model is thus able to capture a stochastic skew, which is e.g. observed for options on currencies.

This is also discussed by Carr and Wu (2004). They use two Lévy processes with jumps, and for both of these processes, they introduce a stochastic time change to capture stochastic volatility. Their parametrization indeed gives rise to a stochastic skew. The main idea to achieve this, however, is not the use of Lévy processes. Rather, it is the stochastic weighting of two components which create an upward and a downward sloping smile, respectively. When the weights change, the slope of the smile changes, and over time, we can thus observe both upward-sloping and downward-sloping smiles.

We first consider the impact of $\rho^{(1)}$ and $\rho^{(2)}$ on the smile, where we assume that all other parameters for the two volatility processes are equal, i.e. $\kappa^{(1)} = \kappa^{(2)}$, $\theta^{(1)} = \theta^{(2)}$ and $\sigma_V^{(1)} = \sigma_V^{(2)}$. Then, the local correlation between stock returns and local variance is a weighted average of $\rho^{(1)}$ and $\rho^{(2)}$

$$\frac{V_t^{(1)}}{V_t^{(1)} + V_t^{(2)}} \rho^{(1)} + \frac{V_t^{(1)}}{V_t^{(1)} + V_t^{(2)}} \rho^{(2)}. \tag{11}$$

The skewness is thus stochastic, and the weights of $\rho^{(1)}$ and $\rho^{(2)}$ depend on the current values of the two local variances $V^{(1)}$ and $V^{(2)}$.

For the following examples, we rely on the parameter set used for the model of Heston (1993) in Section 3.1. We set $\kappa^{(i)} = 1.5$, $\theta^{(i)} = 0.25^2/2$, $\sigma_V^{(i)} = 0.75$ and we set the local

variances $V^{(i)}$ equal to their long run means. For $\rho^{(1)} = \rho^{(2)} = -0.5$, the two-factor model reduces to the model of Heston (1993). Alternatively, we set $\rho^{(1)} = -0.5$ and $\rho^{(2)} = 0.5$, so that the first stochastic volatility process implies a downward sloping smile, while the second one generates an increasing implied volatility curve. The form of the smile then depends on the weights of the two components over the time to maturity of the options , and these weights depend on the current local variances $V^{(i)}$ and $V^{(2)}$ and on their long run means.

Figure 12 shows the impact of the local variances. We fix the total local variance at $\theta^{(1)} + \theta^{(2)}$. For a large $V_0^{(1)}$ and a small $V_0^{(2)}$, the weight of the first, negative correlation in (11) is high, resulting in a negative local correlation and thus in a downward sloping smile. For a small $V_0^{(1)}$ and a large $V_0^{(2)}$, the argument is completely analogous, and for $V_0^{(1)} = V_0^{(2)}$, the local correlation is zero, with a symmetric smile.

The impact of the long run means $\theta^{(1)}$ and $\theta^{(2)}$ is analyzed in Figure 13. We fix the sum $\theta^{(1)} + \theta^{(2)}$, and then change the two long run means $\theta^{(1)}$ and $\theta^{(2)}$. They determine the average weights of the two processes. The larger $\theta^{(1)}$ relative to $\theta^{(2)}$, the larger on average $V^{(1)}$ relative to $V^{(2)}$, and the larger the average weight of the negative correlation $\rho^{(1)}$. First, this implies that we will more often see a negative rather than a positive local correlation, yielding a downward sloping smile more frequently. Second, for long times to maturity, the average correlation is negative, so that the smile tends to be downward sloping, as can be seen in Figure 13.

A comparison of Figures 12 and 13 shows that the impact of the local variances and their long run means depends on the time to maturity. For short times to maturity, the local variance is more important, since there is not much time for the processes to be pulled back towards their long run means. For long times to maturity, however, the long run mean is more important, since it becomes the main determinant of the average correlation of stock returns and the total local variance.

5 Conclusion

Model specification is one of the most important questions in the area of derivatives. A large number of option pricing models has been discussed in the literature. In this study, we focus on models with stochastic volatility and/or stochastic jumps. We analyze which properties of the smile can be explained by these models, and we show how the form of the smile depends on the respective parameters.

We first provide a detailed analysis of the two basic models of Heston (1993) and Merton (1976). The skewness of the smile depends on the correlation between stochastic variance and stock returns or, in case of SJ, on the sign of the expected jumps. The overall level of the implied volatility function depends on the stochastic variance and its long run mean or on the size of the diffusion volatility and the jump intensity. Finally, the curvature of the smile is mainly driven by the volatility of volatility (in case of SV) or by the volatility of the jumps and the weight of the jump component (in case of SJ). The main difference between SV and SJ is the behaviour of the smile for different times to maturity. The impact of the time to maturity is much larger in case of SJ than in case of SV.

In a second step, one can combine the basic models to obtain more sophisticated models. The behaviour of the smile in the model of Bakshi, Cao, and Chen (1997) mainly depends on the relative weights of the diffusion component driven by stochastic volatility and the jump component. A two-factor model for stochastic volatility, as proposed by Bates (2000), is able to explain a stochastic skew which is seen, for example, for currency options.

The paper has analyzed the differences between the models in the pricing of European options. There are several directions for further research. First, one can extend the analysis of pricing differences to other claims like American options or exotic options. In particular, it would be interesting to compare the prices of these options for models that do not differ significantly in the pricing of European options. A second topic is to hedging. Given that we want to use a model for hedging, it is of interest to know the differences between the sensitivities to the risk factors and the differences between the hedging strategies implied by different models. Here, the focus would again be on the differences between models that cannot be distinguished on the basis of the prices of European options.

References

Bakshi, G., C. Cao, and Z. Chen, 1997, Empirical Performance of Alternative Option Pricing Models, *Journal of Finance* 52, 2003–2049.

Bakshi, G., and N. Kapadia, 2003, Delta-Hedged Gains and the Negative Market Volatility Risk Premium, *Review of Financial Studies* 16, 527–566.

Bakshi, G., and D. Madan, 2000, Spanning and Derivative-Security Valuation, *Journal of Financial Economics* 55, 205–238.

Bates, D.S., 1996, Jumps and Stochastic Volatility: Exchange Rate Processes Implicit in Deutsche Mark Options, *Review of Financial Studies* 9, 69–107.

Bates, D.S., 1997, The Skewness Premium: Option Pricing Under Asymmetric Information, *Advances in Futures and Options Research* 9, 51–82.

Bates, D.S., 2000, Post-'87 Crash Fears in the S&P Futures Option Market, *Journal of Econometrics* 94, 181–238.

Bingham, N.H., and R. Kiesel, 1998, *Risk-Neutral Valuation: Pricing and Hedging of Financial Derivatives*. (Springer London).

Black, F., and M. Scholes, 1973, The Pricing of Options and Corporate Liabilities, *Journal of Political Economy* 81, 637–654.

Broadie, M., M. Chernov, and M. Johannes, 2004, Model Specification and Risk Premiums: The Evidence From Futures Options, Working Paper.

Buraschi, A., and J. Jackwerth, 2001, The Price of a Smile: Hedging and Spanning in Option Markets, *Review of Financial Studies* 14, 495–527.

Carr, P., and D. Madan, 2001, Optimal Positioning in Derivative Securities, *Quantitative Finance* 1, 19–37.

Carr, P., and L. Wu, 2003, What Type of Process Underlies Options? A Simple Robust Test, *Journal of Finance* 58, 2581 – 2610.

Carr, P., and L. Wu, 2004, Stochastic Skew in Currency Options, Working Paper.

Coval, J.D., and T. Shumway, 2001, Expected Options Returns, *Journal of Finance* 56, 983–1009.

Cox, J.C., J.E. Ingersoll, and S.A. Ross, 1985, A Theory of the Term Structure of Interest Rates, *Econometrica* 53, 385–407.

Das, S. R., and R. K. Sundaram, 1999, Of Smiles and Smirks: A Term Structure Perspective, *Journal of Financial and Quantitative Analysis* 34, 211–240.

Duffie, D., 2001, *Dynamic Asset Pricing Theory*. (3. ed., Princeton University Press Princeton).

Duffie, D., J. Pan, and K. Singleton, 2000, Transform Analysis and Asset Pricing for Affine Jump Diffusions, *Econometrica* 68, 1343–1376.

Eraker, B., 2004, Do Stock Prices and Volatility Jump? Reconciling Evidence from Spot and Option Prices, *Journal of Finance* 59, 1367–1404.

Eraker, B., M. Johannes, and N. Polson, 2003, The Impact of Jumps in Volatility and Returns, *Journal of Finance* 58, 1269–1300.

Henderson, V., D. Hobson, S. Howison, and T. Kluge, 2004, A Comparison of q-Optimal Option Prices in a Stochastic Volatility Model with Correlation, forthcoming, Review of Derivatives Research.

Heston, S.L., 1993, A Closed-Form Solution for Options with Stochastic Volatility with Applications to Bond and Currency Options, *Review of Financial Studies* 6, 327–343.

Hull, J., and A. White, 1987, The Pricing of Options on Assets with Stochastic Volatilites, *Journal of Finance* 42, 281–300.

Merton, R.C., 1976, Option Pricing When Underlying Stock Returns are Discontinuous, *Journal of Financial Economics* 3, 125–144.

Pan, J., 2002, The Jump-Risk Premia Implicit in Options: Evidence from an Integrated Time-Series Study, *Journal of Financial Economics* 63, 3–50.

Schöbel, R., and J. Zhu, 1999, Stochastic Volatility With an Ornstein-Uhlenbeck Process: An Extension, *European Finance Review* 3, 23–46.

A Appendix

A.1 The Model of Heston (1993)

To price derivatives, one possible way is to solve a partial differential equation. In the model of Heston (1993), the partial differential equation for the claim price $C_t = c(t, s, v, \ldots)$ is

$$\frac{\partial c}{\partial t} + \frac{\partial c}{\partial s}\, rs + \frac{\partial c}{\partial v}\, \kappa(\theta - v) + \frac{1}{2}\, \frac{\partial^2 c}{\partial s^2}\, vs^2 + \frac{1}{2}\, \frac{\partial^2 c}{\partial v^2}\, \sigma_V^2 v + \frac{\partial^2 c}{\partial s \partial v}\, \sigma_V \rho v s \;\; = \;\; rc,$$

and the terminal condition is given by the payoff of the claim at time T. The other possibility is to solve for the risk-neutral expectation (1) of the normalized payoff. In the model of Heston (1993), there is no closed form solution for the risk-neutral density, and Heston (1993) shows how to use characteristic functions and the technique of Fourier inversion to calculate the option price. Here, we rely on the approach used by Bakshi and Madan (2000) and by Duffie, Pan, and Singleton (2000). In the model of Heston (1993), there is a closed form solution for this Fourier transform:

$$E^Q\left[e^{-r(T-t)} e^{iu \ln S_T} | \mathcal{F}_t\right] \;\; = \;\; \exp\left\{\alpha(u, T-t) + iu \ln S_t + \gamma(u, T-t) V_t\right\}$$

where

$$\begin{aligned} \alpha(u,\tau) &= r(iu-1)\tau + \frac{\kappa\theta}{\sigma_V^2}\left(2\ln\frac{2\delta}{2\delta + (g(u)-\delta)\left(1-e^{-\delta\tau}\right)} + (g(u)-\delta)\,\tau\right) \\ \gamma(u,\tau) &= \frac{iu(iu-1)\left(1-e^{-\delta\tau}\right)}{2\delta + (g(u)-\delta)\left(1-e^{-\delta\tau}\right)}. \end{aligned}$$

and where

$$\begin{aligned} g(u) &= \kappa - iu\rho\sigma_V \\ \delta &= \sqrt{g(u)^2 - iu(iu-1)\sigma_V^2} \end{aligned}$$

Given this formula, the price of a call option can be calculated by numerical integration as shown in Equation (3).

A.2 The Model of Merton (1976)

In the model of Merton (1976), the partial differential equation for the price $C_t = c(t, s, \ldots)$ of a European claim is

$$\frac{\partial c}{\partial t} + \frac{\partial c}{\partial s}\, \left(r - E^Q[e^X - 1]\lambda_0\right) s + \frac{1}{2}\, \frac{\partial^2 c}{\partial s^2}\, \sigma^2 s^2 + E^Q\left[c(t, se^X, \ldots) - c(t, s, \ldots)\right] \lambda_0 \;\; = \;\; rc,$$

where the expectation of the jump in the claim price is taken over the jump size X. The terminal condition is given by the payoff function of the claim to be priced.

An alternative way to calculate the price of a European contingent claim is to use Fourier inversion. The Fourier transform (2) of the state price density is

$$E^Q\left[e^{-r(T-t)}e^{iu\ln S_T}|\mathcal{F}_t\right] \;=\; \exp\left\{\alpha(u,T-t)+iu\ln S_t\right\},$$

where

$$\alpha(u,\tau) \;=\; r(iu-1)\tau+0.5iu(iu-1)\sigma^2-\left(E^Q[e^X-1]iu-E[e^{iuX}-1]\right)\lambda_0\tau.$$

A.3 The Model of Bakshi, Cao, and Chen (1997)

The partial differential equation for the claim price $C_t=c(t,s,v,\ldots)$ is

$$\begin{aligned}&\frac{\partial c}{\partial t}+\frac{\partial c}{\partial s}\left(r-E^Q[e^X-1]\lambda_0\right)s+\frac{\partial c}{\partial v}\,\kappa(\theta-v)\\ &+\frac{1}{2}\,\frac{\partial^2 c}{\partial s^2}\,vs^2+\frac{1}{2}\,\frac{\partial^2 c}{\partial v^2}\,\sigma_V^2 v+\frac{\partial^2 c}{\partial s\partial v}\,\sigma_V\rho vs+E^Q\left[c(t,se^X,\ldots)-c(t,s,\ldots)\right]\lambda_0 \;=\; rc\end{aligned}$$

where the expectation of the differences in the prices before and after a jump is computed with respect to the jump size X.

The Fourier transform (2) of state price density can again be calculated in closed form. It is given by

$$E^Q\left[e^{-r(T-t)}e^{iu\ln S_T}|\mathcal{F}_t\right] \;=\; \exp\left\{\alpha(u,T-t)+iu\ln S_t+\gamma(u,T-t)V_t\right\}$$

where

$$\begin{aligned}\alpha(u,\tau) \;&=\; r(iu-1)\tau-\left(E^Q[e^X-1]iu-E^Q[e^{iuX}-1]\right)\lambda_0\tau\\ &\quad+\frac{\kappa\theta}{\sigma_V^2}\left\{2\ln\frac{2\delta}{2\delta+(g(u)-\delta)(1-e^{-\delta\tau})}+(g(u)-\delta)\,\tau\right\}\\ \gamma(u,\tau) \;&=\; \frac{iu(iu-1)(1-e^{-\delta\tau})}{2\delta+(g(u)-\delta)(1-e^{-\delta\tau})}\end{aligned}$$

and

$$\begin{aligned}g(u) \;&=\; \kappa-iu\rho\sigma_V\\ \delta \;&=\; \sqrt{g(u)^2-iu(iu-1)\sigma_V^2}.\end{aligned}$$

A.4 SVJ Model with Volatility-Dependent Jump Intensity

The partial differential equation for the claim price $C_t = c(t, s, v, \ldots)$ is

$$\begin{aligned} & \frac{\partial c}{\partial t} + \frac{\partial c}{\partial s}\ \left(r - E^Q[e^X - 1]\lambda_1 V_t\right) s + \frac{\partial c}{\partial v}\ \kappa(\theta - v) \\ + \frac{1}{2}\ \frac{\partial^2 c}{\partial s^2}\ vs^2 + \frac{1}{2}\ \frac{\partial^2 c}{\partial v^2}\ \sigma_V^2 v + \frac{\partial^2 c}{\partial s \partial v}\ \sigma_V \rho v s + E^Q\left[c(t, se^X, \ldots) - c(t, s, \ldots)\right] \lambda_1 V_t &= rc \end{aligned}$$

where the expectation of the differences in the prices before and after a jump is computed with respect to the jump size X.

The Fourier transform (2) of the state price density is

$$E^Q\left[e^{-r(T-t)} e^{iu \ln S_T} | \mathcal{F}_t\right] = \exp\left\{\alpha(u, T-t) + iu \ln S_t + \gamma(u, T-t) V_t\right\}$$

where

$$\begin{aligned} \alpha(u, \tau) &= (iu - 1) r\tau + \frac{\kappa\theta}{\sigma_V^2}\left\{2 \ln \frac{2\delta}{2\delta + (g(u) - \delta)(1 - e^{-\delta\tau})} + (g(u) - \delta)\,\tau\right\} \\ \gamma(u, \tau) &= \frac{\left[iu(iu-1) - 2\left(E^Q[e^X - 1]iu - E^Q[e^{iuX} - 1]\right)\lambda_1\right](1 - e^{-\delta\tau})}{2\delta + (g(u) - \delta)(1 - e^{-\delta\tau})} \end{aligned}$$

and

$$\begin{aligned} g(u) &= \kappa - iu\rho\sigma_V \\ \delta &= \sqrt{g(u)^2 - iu(iu-1)\sigma_V^2 + 2\left(E^Q[e^X - 1]iu - E^Q[e^{iuX} - 1]\right)\lambda_1 \sigma_V^2}. \end{aligned}$$

A.5 Two-Factor Stochastic Volatility Model

The partial differential equation for the claim price $C_t = c(t, s, v, \ldots)$ is

$$\begin{aligned} & \frac{\partial c}{\partial t} + \frac{\partial c}{\partial s}\ rs + \frac{1}{2}\ \frac{\partial^2 c}{\partial s^2}\ \left(\left(v^{(1)}\right)^2 + \left(v^{(2)}\right)^2\right) s^2 \\ + \frac{\partial c}{\partial v^{(1)}}\ \kappa^{(1)}\left(\theta^{(1)} - v^{(1)}\right) + \frac{1}{2}\ \frac{\partial^2 c}{\partial \left(v^{(1)}\right)^2}\ \left(\sigma_V^{(1)}\right)^2 v^{(1)} + \frac{\partial^2 c}{\partial s \partial v^{(1)}}\ \sigma_V^{(1)} \rho^{(1)} v^{(1)} s \\ + \frac{\partial c}{\partial v^{(2)}}\ \kappa^{(2)}\left(\theta^{(2)} - v^{(2)}\right) + \frac{1}{2}\ \frac{\partial^2 c}{\partial \left(v^{(2)}\right)^2}\ \left(\sigma_V^{(2)}\right)^2 v^{(2)} + \frac{\partial^2 c}{\partial s \partial v^{(2)}}\ \sigma_V^{(2)} \rho^{(2)} v^{(2)} s &= rc, \end{aligned}$$

and the terminal condition is given by the payoff of the claim at time T.

The Fourier transform is very similar to the one in case of the Heston (1993) model. We get

$$\begin{aligned} & E^Q\left[e^{-r(T-t)} e^{iu \ln S_T} | \mathcal{F}_t\right] \\ &= \exp\left\{\alpha_{1+2}(u, T-t) + iu \ln S_t + \gamma_1(u, T-t) V_t^{(1)} + \gamma_2(u, T-t) V_t^{(2)}\right\}, \end{aligned}$$

where

$$\begin{aligned}
\alpha_{1+2}(u,\tau) &= r(iu-1)\tau \\
&\quad + \frac{\kappa^{(1)}\theta^{(1)}}{\left(\sigma_V^{(1)}\right)^2}\left(2\ln\frac{2\delta^{(1)}}{2\delta^{(1)}+\left(g_1(u)-\delta^{(1)}\right)\left(1-e^{-\delta^{(1)}\tau}\right)}+\left(g_1(u)-\delta^{(1)}\right)\tau\right) \\
&\quad + \frac{\kappa^{(2)}\theta^{(2)}}{\left(\sigma_V^{(2)}\right)^2}\left(2\ln\frac{2\delta^{(2)}}{2\delta^{(2)}+\left(g_2(u)-\delta^{(2)}\right)\left(1-e^{-\delta^{(2)}\tau}\right)}+\left(g_2(u)-\delta^{(2)}\right)\tau\right) \\
\gamma_1(u,\tau) &= \frac{iu(iu-1)\left(1-e^{-\delta^{(1)}\tau}\right)}{2\delta^{(1)}+\left(g_1(u)-\delta^{(1)}\right)\left(1-e^{-\delta^{(1)}\tau}\right)} \\
\gamma_2(u,\tau) &= \frac{iu(iu-1)\left(1-e^{-\delta^{(2)}\tau}\right)}{2\delta^{(2)}+\left(g_2(u)-\delta^{(2)}\right)\left(1-e^{-\delta^{(2)}\tau}\right)}
\end{aligned}$$

and

$$\begin{aligned}
g_1(u) &= \kappa^{(1)}-iu\rho^{(1)}\sigma_V^{(1)} \\
g_2(u) &= \kappa^{(2)}-iu\rho^{(2)}\sigma_V^{(2)} \\
\delta^{(1)} &= \sqrt{g_1(u)^2-iu(iu-1)\left(\sigma_V^{(1)}\right)^2} \\
\delta^{(2)} &= \sqrt{g_2(u)^2-iu(iu-1)\left(\sigma_V^{(2)}\right)^2}.
\end{aligned}$$

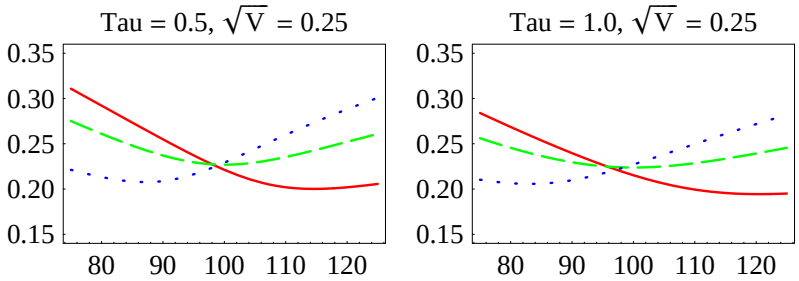

Figure 1: Heston Model: Impact of Correlation ρ

The graphs shows the impact of the correlation ρ between the stock and the local variance on the implied volatility as a function of the strike price. The current stock price is 100, the risk free rate is 0. In the base case, $\kappa = 1.5$, $\theta = 0.25^2$, $\sigma_V = 0.75$, $\rho = -0.5$, and V is equal to its long run mean. This base case is the solid line in each graph.

The correlation ρ is equal to -0.5 (solid line), 0 (dashed line) and 0.5 (dotted line). The time to maturity of the options is six months (left graph) and one year (right graph).

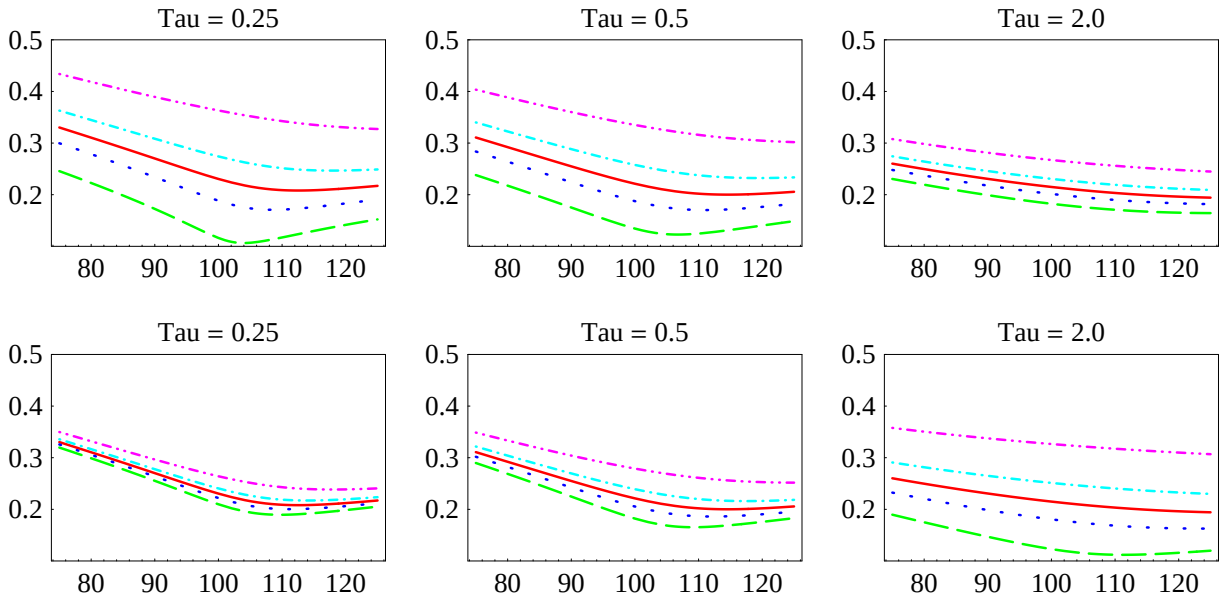

Figure 2: Heston Model: Impact of local variance V and of its long run mean θ

The graphs show the impact of the local variance V (upper row) and its long-run mean θ (lower row) on the implied volatility as a function of the strike price. The current stock price is 100, the risk free rate is 0. In the base case, $\kappa = 1.5$, $\theta = 0.25^2$, $\sigma_V = 0.75$, $\rho = -0.5$, and the local variance V is equal to its long run mean θ. This base case is the solid line in each graph.

In the upper row, local variance is (from bottom to top) equal to $0.1^2, 0.20^2, 0.25^2, 0.30^2, 0.40^2$, and in the lower row, the long run mean θ is (from bottom to top) equal to $0.1^2, 0.20^2, 0.25^2, 0.30^2, 0.40^2$. The time to maturity of the options is three months (left column), six months (middle column) and two years (right column).

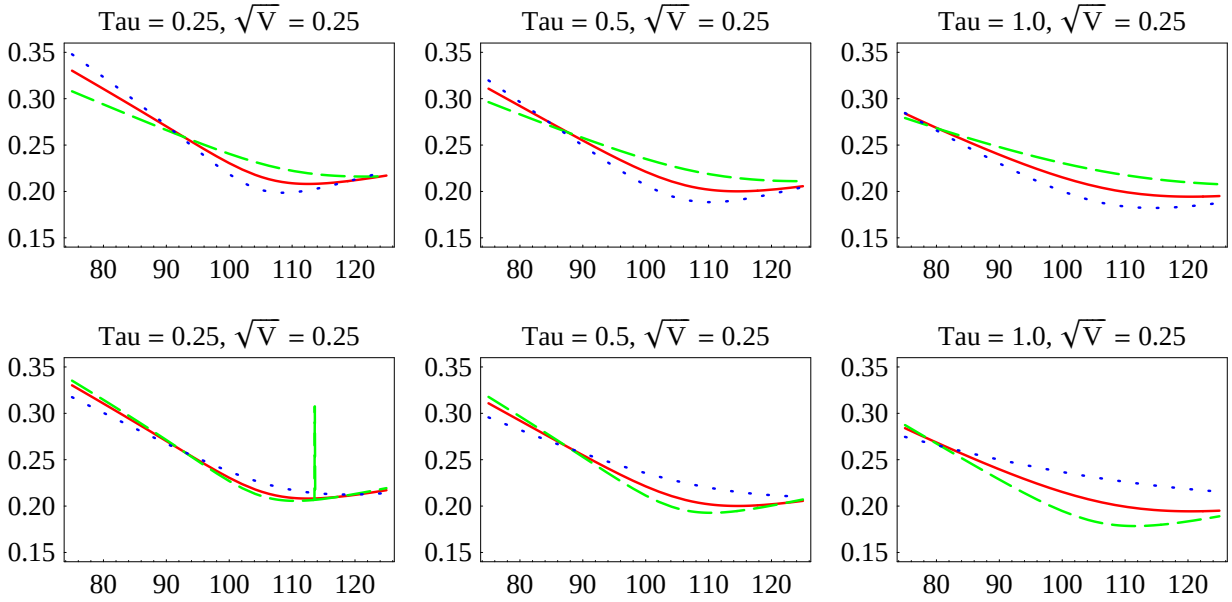

Figure 3: Heston Model: Impact of volatility of volatility σ_V and of κ for different times to maturity

The graphs show the impact of the volatility of volatility σ_V (upper row) and of the mean reversion speed κ (lower row) for different times to maturity on the implied volatility as a function of the strike price. The current stock price is 100, the risk free rate is 0. In the base case, $\kappa = 1.5$, $\theta = 0.25^2$, $\sigma_V = 0.75$, $\rho = -0.5$, and V is equal to its long run mean. This base case is the solid line in each graph.

In the upper row, volatility of volatility σ_V is equal to 0.5 (dashed line), 0.75 (solid line), and 1.0 (dotted line). In the lower row, the mean reversion speed κ is equal to 0.5 (dashed line), 1.5 (solid line), and 4.5 (dotted line). The time to maturity of the options is 0.25, 0.5 and 1.0 (from left to right).

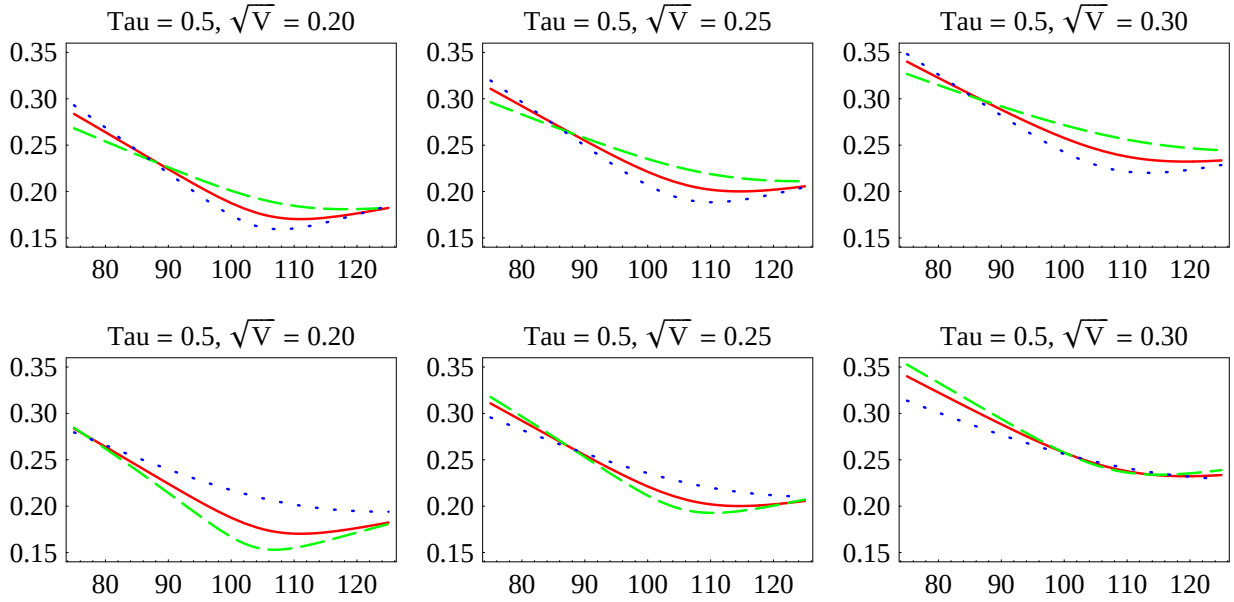

Figure 4: Heston Model: Impact of volatility of volatility σ_V and of κ for different values of the local variance V

The graphs show the impact of the volatility of volatility σ_V (upper row) and of the mean reversion speed κ (lower row) for different values of the local variance V on the implied volatility as a function of the strike price. The current stock price is 100, the risk free rate is 0. In the base case, $\kappa = 1.5$, $\theta = 0.25^2$, $\sigma_V = 0.75$, $\rho = -0.5$, and time to maturity is 0.5. This base case is the solid line in each graph.

In the upper row, volatility of volatility σ_V is equal to 0.5 (dashed line), 0.75 (solid line), and 1.0 (dotted line). In the lower row, the mean reversion speed κ is equal to 0.5 (dashed line), 1.5 (solid line), and 4.5 (dotted line). The local variance V is below its long run mean (left column), equal to its long run mean (middle column), and above its long run mean (right column).

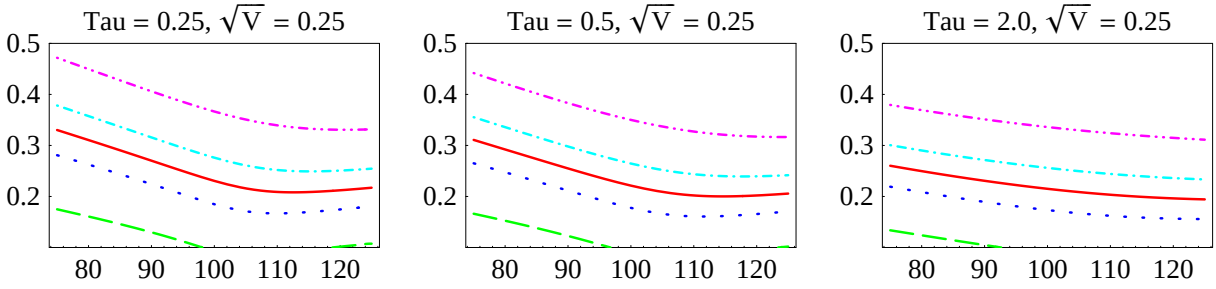

Figure 5: Heston Model: Scaling of Stochastic Volatility

The graphs show the impact of the scaling factor for stochastic volatility on the implied volatility as a function of the strike price. The current stock price is 100, the risk free rate is 0.0. In the base case, $\kappa = 1.5$, $\theta = 0.25^2$, $\sigma_V = 0.75$, $\rho = -0.5$, and V is equal to its long run mean. This base case is the solid line in each graph.

The scaling factor α for the local volatility is $0.4, 0.8, 1.0, 1.2, 1.6$ (from bottom to top), so that the local volatility is $0.10, 0.20, 0.25, 0.30, 0.40$ (from bottom to top). The time to maturity of the options is 0.25, 0.5 and 2.0 (from left to right).

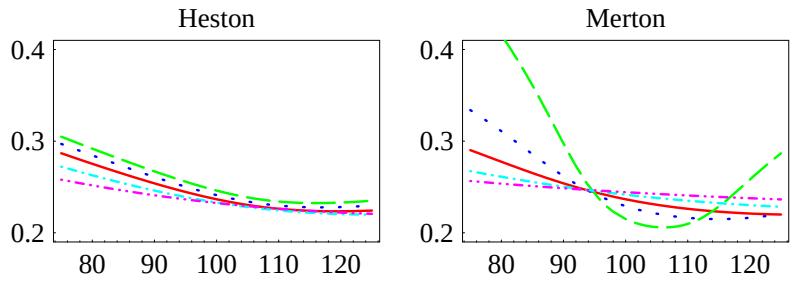

Figure 6: Merton Model and Heston Model: Impact of Time to Maturity

The graphs show the impact of the time to maturity for SV and SJ on the implied volatility as a function of the strike price. The current stock price is 100, the risk free rate is 0. The parameters in the SJ model of Merton (1976) are $\sigma = 0.18$, $\lambda_0 = 0.897556$, $\mu_X = -0.1$, and $\sigma_X = 0.15$. The SV model of Heston (1993) is calibrated to the prices of European options as calculated in the model of Merton (1976) with six months to maturity and strike prices between 90 and 110 (the relative pricing errors are below 0.3%). The implied volatility function for a time to maturity of six months is the solid line in each graph.

The left graph shows the impact of the time to maturity in the model of Heston (1993), the right graph shows the impact in the model of Merton (1976). The times to maturity are $1, 3, 6, 12$, and 24 months, and the larger the time to maturity, the flatter the smile in both models.

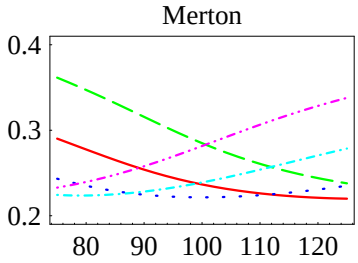

Figure 7: Merton Model: Impact of average jump size μ_X in log return

The graphs show the impact of mean jump size μ_X on the implied volatility as a function of the strike price. The current stock price is 100, the risk free rate is 0. In the base case, $\sigma = 0.18$, $\lambda_0 = 0.897556$, $\mu_X = -0.1$, and $\sigma_X = 0.15$, and the time to maturity is six months. This base case is the solid line in each graph.

The mean jump size μ_X is -0.2 (dashed line), -0.1 (solid line), 0.0 (dotted line), 0.1 (single-dash-dotted line), and 0.2 (double dash-dotted line).

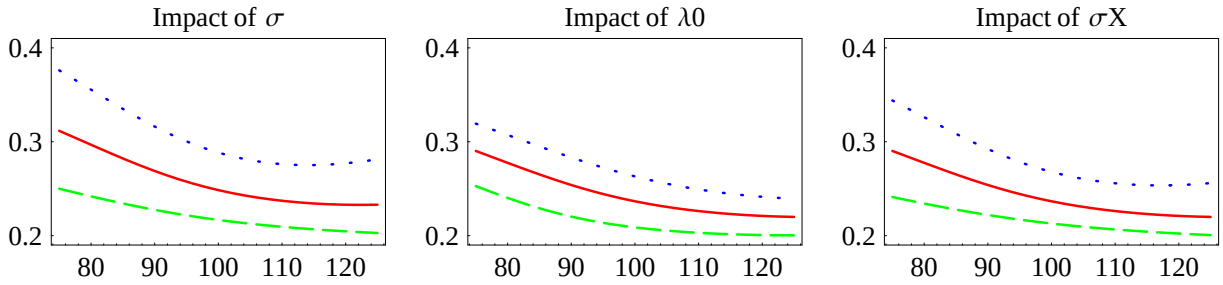

Figure 8: Merton Model: Impact of volatility, jump intensity and jump volatility

The graphs show the impact of the diffusion volatility σ (left graph), the jump intensity λ_0 (middle graph), and the jump volatility σ_X (right graph) on the implied volatility as a function of the strike price. The current stock price is 100, the risk free rate is 0. In the base case, $\sigma = 0.18$, $\lambda_0 = 0.897556$, $\mu_X = -0.1$, and $\sigma_X = 0.15$, and the time to maturity is six months. This base case is the solid line in each graph.

In each graph, the parameter is either halved (dashed line) or doubled (dotted line).

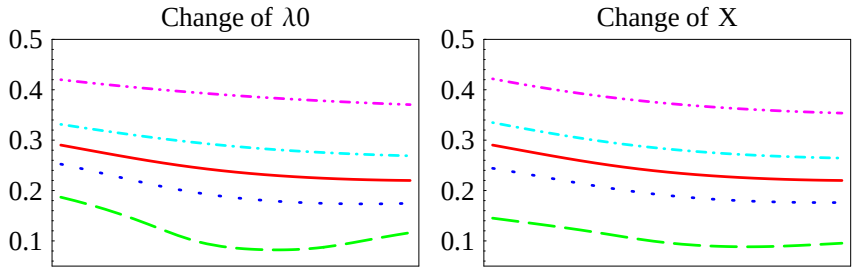

2

Figure 9: Merton Model: Scaling of Local Variance

The graphs show the impact of the scaling factor for local variance on the implied volatility as a function of the strike price. The current stock price is 100, the risk free rate is 0. In the base case, $\sigma = 0.18$, $\lambda_0 = 0.897556$, $\mu_X = -0.1$, and $\sigma_X = 0.15$, and the time to maturity is six months. This base case is the solid line in each graph.

The scaling factor α for the local volatility is $0.4, 0.8, 1.0, 1.2, 1.6$ (from bottom to top). The diffusion volatility σ is replaced by $\widetilde{\sigma} = \alpha\sigma$. In the left graph, the jump intensity λ_0 is replaced by $\widetilde{\lambda}_0 = \alpha^2\lambda_0$, in the right graph, the jump size X is replaced by $\widetilde{X} = \alpha X$.

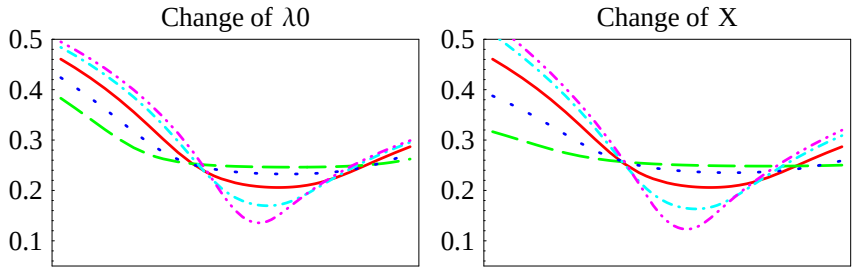

Figure 10: Merton Model: Impact of jumpiness

The graphs show the impact of the jumpiness on the implied volatility as a function of the strike price. The current stock price is 100, the risk free rate is 0. In the base case, $\sigma = 0.18$, $\lambda_0 = 0.897556$, $\mu_X = -0.1$, and $\sigma_X = 0.15$, and the time to maturity is one month. This base case with a jumpiness of 0.5 is the solid line in each graph.

The jumpiness is equal to 0.1 (dashed line), 0.25 (dotted line), 0.5 (solid line), 0.75 (single dash-dotted line) and 0.9 (double dash-dotted line), and the larger the jumpiness, the steeper the smile. In the left graph, the jump intensity λ_0 is adjusted, in the right graph, the jump size is adjusted.

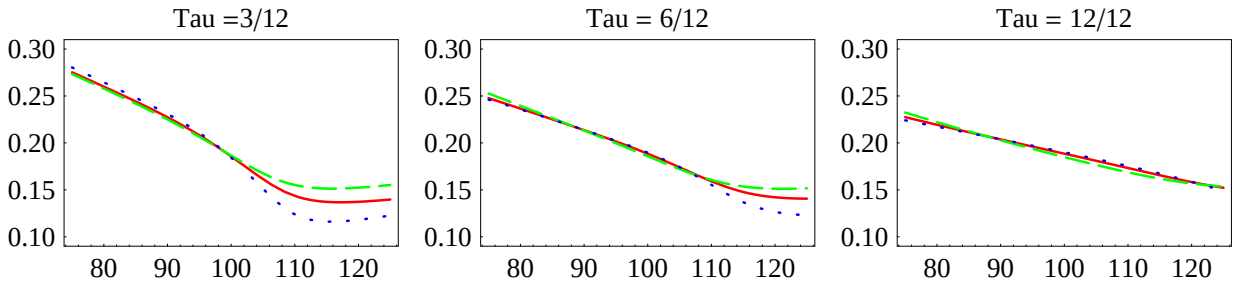

Figure 11: BCC Model: Impact of jumpiness

The graphs show the impact of the jumpiness on the implied volatility for different times to maturity as a function of the strike price. The current stock price is 100, the risk free rate is 0. In the base case, $\theta = \frac{0.04}{2.03}$, $\kappa = 2.03$, $\sigma_V = 0.38$, $\rho = -0.57$, $\lambda_0 = 1.1925$, $\mu_X = -0.10$, $\sigma_X = 0.07$, and V is equal to its long run mean. This base case with a jumpiness of 0.5 is the solid line in each graph.

Jumpiness is equal to 0.25 (dashed line), 0.5 (solid line), and 0.75 (dotted line). The time to maturity of the options is 3, 6 and 12 months (from left to right).

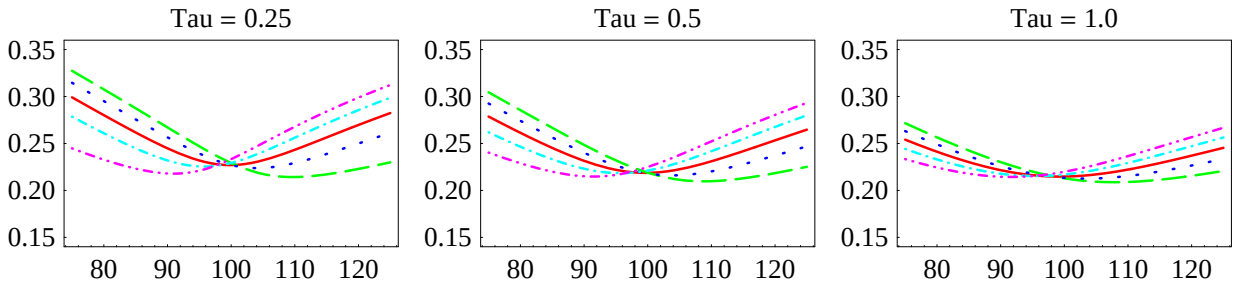

Figure 12: Two-Factor SV-Model: Impact of current local variances

The graphs show the impact of the relative weights of the two stochastic volatility processes for different times to maturity on the implied volatility as a function of the strike price. The current stock price is 100, the risk free rate is 0. In the base case, the parameters of the SV processes are $\kappa^{(i)} = 1.5$, $\theta^{(i)} = 0.25^2/2$ and $\sigma_V^{(i)} = 0.75$ for $i = 1, 2$, the correlations are $\rho^{(1)} = -0.5$ and $\rho^{(2)} = 0.5$, and $V^{(1)}$ and $V^{(2)}$ are both equal to their long run means. This base case is the solid line in each graph.

The sum $V = V^{(1)} + V^{(2)}$ is fixed, and the weights of the two processes are changed by setting $V^{(1)}$ equal to 0 (double dash-dotted line), $0.25V$ (dash-dotted line), $0.5V$ (solid line), $0.75V$ (dotted line) and V (dashed line). The time to maturity of the options is 0.25, 0.5 and 1.0 year (from left to right).

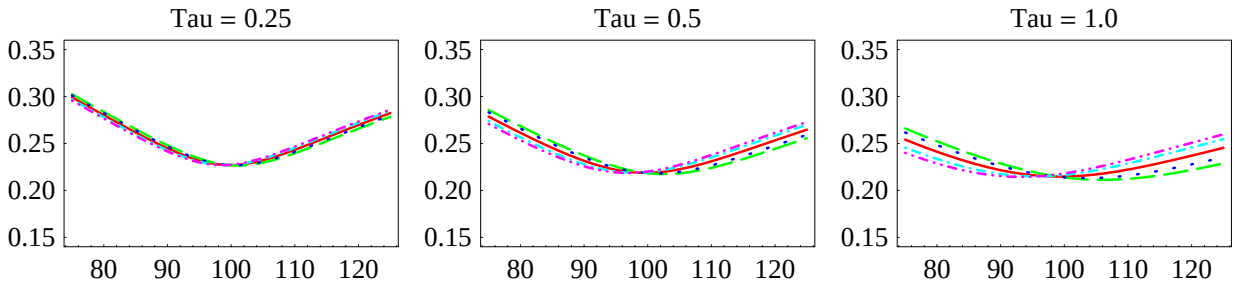

Figure 13: Two-Factor SV-Model: Impact of long run means of local variances

The graphs show the impact of the long run means of the two stochastic volatility processes for different times to maturity on the implied volatility as a function of the strike price. The current stock price is 100, the risk free rate is 0. In the base case, the parameters of the SV processes are $\kappa^{(i)} = 1.5$, $\theta^{(i)} = 0.25^2/2$ and $\sigma_V^{(i)} = 0.75$ for $i = 1, 2$, the correlations are $\rho^{(1)} = -0.5$ and $\rho^{(2)} = 0.5$, and $V^{(1)}$ and $V^{(2)}$ are both equal to their long run means. This base case is the solid line in each graph.

The sum $\theta = \theta^{(1)} + \theta^{(2)}$ is fixed, and the weights of the two processes are changed by setting $\theta^{(1)}$ equal to 0.1θ (double dash-dotted line), 0.25θ (dash-dotted line), 0.5θ (solid line), 0.75θ (dotted line) and 0.9θ (dashed line). The time to maturity of the options is 0.25, 0.5 and 1.0 year (from left to right).